AD-A085 762 ILLINOIS UNIV AT URBANA-CHAMPAIGN DECISION AND CONTROL LAB F/G 12/1
DESIGN OF OPTIMALLY ROBUST CONTROL SYSTEMS.(U)
JAN 80 C B CHATO N00014-79-C-0424
UNCLASSIFIED DC-34 NL

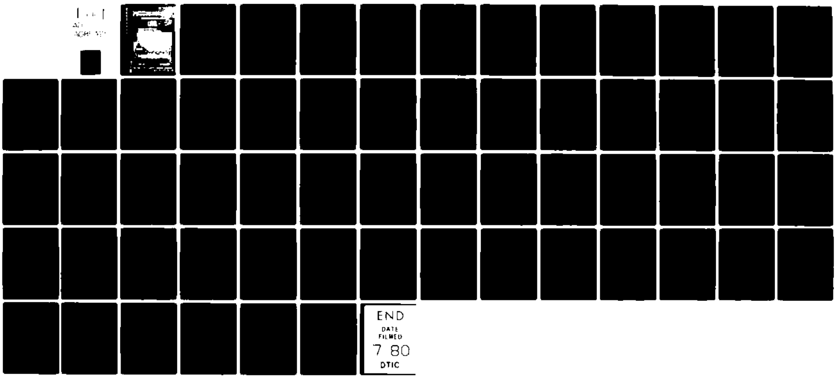

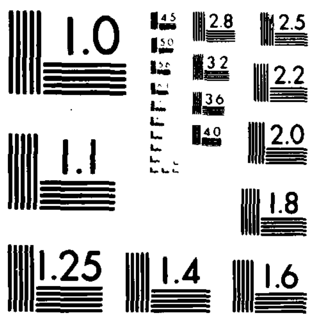

MICROCOPY RESOLUTION TEST CHART
NATIONAL BUREAU OF STANDARDS 1963 A

UNCLASSIFIED

SECURITY CLASSIFICATION OF THIS PAGE (When Data Entered)

REPORT DOCUMENTATION PAGE

READ INSTRUCTIONS BEFORE COMPLETING FORM

1. REPORT NUMBER

2. GOVT ACCESSION NO. AD-A085 762

3. RECIPIENT'S CATALOG NUMBER

4. TITLE (and Subtitle)
(6) DESIGN OF OPTIMALLY ROBUST CONTROL SYSTEMS,

5. TYPE OF REPORT & PERIOD COVERED
Technical Report

6. PERFORMING ORG. REPORT NUMBER
R-870 (DC-34); UILU-80-2202

7. AUTHOR(s)
(10) CHRISTINE BARBARA CHATO (15)

8. CONTRACT OR GRANT NUMBER(s)
N00014-79-C-0424

9. PERFORMING ORGANIZATION NAME AND ADDRESS
Coordinated Science Laboratory
University of Illinois at Urbana-Champaign
Urbana, Illinois 61801
(9)

10. PROGRAM ELEMENT, PROJECT, TASK AREA & WORK UNIT NUMBERS
Master's thesis

11. CONTROLLING OFFICE NAME AND ADDRESS
Joint Services Electronics Program
(11)

12. REPORT DATE
Jan[redacted]80

13. NUMBER OF PAGES
52

14. MONITORING AGENCY NAME & ADDRESS (if different from Controlling Office)
(14) DC-34, UILU-ENG-80-2203

15. SECURITY CLASS. (of this report)

15a. DECLASSIFICATION/DOWNGRADING SCHEDULE

16. DISTRIBUTION STATEMENT (of this Report)

Approved for public release; distribution unlimited. (12) 64

17. DISTRIBUTION STATEMENT (of the abstract entered in Block 20, if different from Report)

18. SUPPLEMENTARY NOTES

19. KEY WORDS (Continue on reverse side if necessary and identify by block number)
robust control
optimization
output feedback

20. ABSTRACT (Continue on reverse side if necessary and identify by block number)

This thesis develops an approach to the design of constant output feedback controllers for linear systems which incorporates many common approaches. It is assumed that some of the design criteria can be represented as restrictions on the locations of the closed-loop system eigenvalues in the complex plane. Additional constraints are represented by a quadratic cost function. The design problem is then to choose a set of constant output feedback gains that minimize the cost function subject to the constraints.

DD FORM 1 JAN 73 1473 EDITION OF 1 NOV 65 IS OBSOLETE

UNCLASSIFIED 410775

SECURITY CLASSIFICATION OF THIS PAGE (When Data Entered)

UILU-80-2202

DESIGN OF OPTIMALLY ROBUST CONTROL SYSTEMS

by

Christine Barbara Chato

This work was supported in part by the Joint Services Electronics Program (U. S. Army, U. S. Navy, and U. S. Air Force) under Contract N00014-79-C-0424.

DESIGN OF OPTIMALLY ROBUST CONTROL SYSTEMS

BY

CHRISTINE BARBARA CHATO

B.S., University of Illinois, 1978

THESIS

Submitted in partial fulfillment of the requirements
for the degree of Master of Science in Electrical Engineering
in the Graduate College of the
University of Illinois at Urbana-Champaign, 1980

Urbana, Illinois

ACKNOWLEDGMENT

The author wishes to thank her advisor, Professor D. P. Looze, for all his help. Thanks also go to Professor J. E. Ackermann, with special thanks to Norm Franklin, who went through all this before the author did.

TABLE OF CONTENTS

LIST OF FIGURES

LIST OF TABLES

1. INTRODUCTION

This thesis deals with the problem of robust control system design, i.e., a control system which will work in the presence of perturbations in the structure or the parameters of the system. The problem of robust control is important for several reasons. Control systems are typically designed on the basis of linear time-invariant models of real systems. However, they must operate on the actual systems which may be neither linear nor time invariant. Therefore it is important to design a controller which will work even though the system and the model are not identical. Some examples of perturbations to the system which a controller should be able to handle are sensor failures, actuator failures, different operating conditions, and uncertainties in the plant model. This design approach may also be used to determine which sensors are really essential in order to control the system and which are not [1,21].

Two common approaches to robust control system design are adaptive control and fixed gain control. The idea of adaptive control is to continually modify the structure and parameters of the controller in order to achieve the best possible performance given the current information available about the system. One problem with this approach is that inputs to the system which lead to quick and accurate identification do not usually lead to the best system performance. The reverse also holds. The idea behind fixed gain control is to find one fixed gain controller which will work well over a range of system perturbations. In this case, the system performance at any particular point may not be the best possible [1].

The fixed gain output or state feedback controller is the simplest form of controller for the type of systems considered in this thesis. Its simplicity makes this type of controller attractive. If a fixed gain controller can be found such that the design specifications for a given problem can be satisfied for all operating conditions, there is no need for a more complex one. Schy [3] has shown that in many cases a fixed gain controller will be able to accommodate a large variation of system parameters. On the other hand, the fixed gain solution may indicate that a more complicated controller is required. Even in this case, however, the design process which led to that conclusion will have provided insight into the problem and possible solutions [1].

There are many approaches to the design of fixed gain controllers. One frequently used design technique is to represent the design criteria by a quadratic cost function which is then minimized. Formulating the problem as an optimization problem makes the problem computationally tractable. Also, some typical design criteria, such as minimizing the control energy or the control rate, can be easily represented by a linear quadratic cost function. Kalman [4], Anderson and Moore [5], and Safonov and Athans [6] all discuss this approach to designing state feedback regulators. Harvey and Pope [7,8] and Vinkler and Wood [9] compare the behavior of these methods when applied to some aircraft problems. The basic difficulty with this approach is that the optimization framework is an artificial device. While some design constraints can easily be incorporated into a single cost function, many other very common ones such as damping ratios, bandwidth, etc. often cannot easily be represented this way.

Design criteria are often more naturally translated into constraints on the location of the closed loop system eigenvalues in the complex plane or on the location of other system parameters. Sirisena and Choi [2] use a pseudoinverse method to design a constant output controller which places the closed loop system poles in prescribed regions of the complex plane. One problem with their method is that their algorithm could converge to a local minimum outside the constraint region. Also even if the algorithm fails to converge to the minimum for a wide range of initial guesses for the feedback gains, one cannot be absolutely sure that no solution exists. Ackermann [1] maps regions in the complex plane into regions in the space of feedback gains and suggests doing the actual design in the gain space. This method can also be used for finding gains which are robust with respect to known parameter variations. Regions in the complex plane, each representing the constraints for a certain set of parameters, are all mapped into the gain space. The intersection of all these regions is the set of gains for which all the constraints are satisfied. This method has the advantage over the previous one that the designer will be able to see graphically if no solution exists. It has the disadvantage that for systems with more than two or three feedback gains, finding a graphical representation of the whole region of possible gains becomes complicated. In this case, it would be simpler to find one good point rather than the whole region.

Zakian and Al-Naib [10] represent all design criteria as a set of linear inequalities, $\phi_i(\underline{P}) \leq C_i$ where $\underline{P}$ is the vector of system parameters which may be varied and C_i is constant. This formulation yields regions in the parameter space where the parameters must lie. A numerical method of obtaining a solution is presented. This method involves starting with fairly loose constraints (to insure a region of intersection) and making the constraints more stringent at each iteration until an acceptable solution is found. For this formulation, some trial and error is usually necessary to find a realistic set of inequalities [10]. Kreisselmeier and Steinhauser [11] used a similar formulation to design a controller for an F4-C plane. However, they solved the system of inequalities using a min-max optimization method rather than the shrinking boundary method described above.

This thesis develops an approach to the design of constant output feedback controllers for linear systems which incorporates many of the approaches mentioned above. It is assumed that some of the design criteria can be represented as restrictions on the locations of the closed-loop system eigenvalues in the complex plane. Additional constraints are represented by a quadratic cost function. The design problem is then to choose a set of constant output feedback gains that minimize the cost function subject to the constraints. This formulation is most similar to that of Sirisena and Choi [2] except that their cost function is simply a measure of how much the constraints are violated; whereas, for this thesis, the cost function incorporates additional design specifications which are not represented by the constraints.

There are several advantages to this approach. The advantage of using constant output feedback lies in the simplicity of its implementation. Another advantage is that unlike the unconstrained optimization formulation, all the design specifications need not be represented by a single cost function. Those that can be most naturally expressed as regions in the complex plane, such as damping ratios, bandwidth requirements, step responses, etc. are expressed that way. Others, such as minimum energy control, input rate, etc., are represented in the cost function. Whereas some of the previously mentioned constraint methods yield a whole region of acceptable gains, this approach yields a particular point in the region.

The method used to solve the problem is also slightly different from those described above. The problem is first reformulated as an optimization over the feedback gains. Then this optimization problem is solved using an augmented Lagrangian approach.

In Section 2, a precise mathematical formulation of the problem is given. Section 3 discusses the nonlinear programming method which was used to solve the problem. Section 4 derives the gradients which are necessary to solve the problem. In Section 5, a second order numerical example is presented. The purpose of presenting this example is to discuss some of the problems involved in implementing this method. Finally, this approach to controller design is applied to the design of a fixed gain controller for the linearized longitudinal flight dynamics of an F-4 aircraft. Four flight conditions in both normal and failure modes will be considered simultaneously. Design constraints for the normal and failure modes will be assumed to be specified separately. This example was studied by Franklin [12] using Ackermann's mapping technique [1]. The results of both methods are then discussed.

2. THE PROBLEM AND ITS REFORMULATION

The purpose of this section is to present a precise mathematical formulation of the problem discussed in the Introduction of this thesis and then to reformulate the problem in a form that is computationally easier to work with. As mentioned in the Introduction, this thesis deals with the problem of using output feedback to control a fixed structure system. The design problem is to choose the constant feedback gains which are best with respect to some cost function such that the closed loop system satisfies certain design specifications. It is assumed that these design specifications can be represented most naturally as regions in the complex plane where the eigenvalues of the closed loop system must be located. The system is also assumed to be linear time invariant.

The precise problem formulation is as follows:

$$\min_{k\in S} J = \tfrac{1}{2} E\{\int_{o}^{\infty} [x^T(t)Qx(t) + u^T(t)Ru(t)]dt\} \tag{1}$$

subject to

$$\underline{\dot{x}}(t) = A\underline{x}(t) + B\underline{u}(t); \qquad x(t_o) = x_o \tag{2}$$

$$E\{x_o\} = 0; \quad E\{x_o x_o^T\} = X_o$$

$$\underline{y}(t) = C\underline{x}(t) \tag{3}$$

$$u(t) = -K\underline{y}(t) \tag{4}$$

$$g_i(\lambda) \leq 0 \qquad i = 1,\ldots,N \tag{5}$$

where $\underline{x}(t) \in R^n$, $u(t) \in R^m$, and $y(t) \in R^p$. S is the space of permissible feedback gains. The expectation of the integral is used so that the cost, J, is independent of any particular initial state of the system, but depends instead on an average initial condition of all the possible initial states. Q and R are nonnegative definite constant matrices chosen so that given some predetermined criteria, by minimizing J, one is improving the closed loop behavior of the system. For example, if Q is the zero matrix and R is the identity, J represents the total energy used to control the system. By minimizing J, one is minimizing the total energy used. The functions, $g_i(\underline{\lambda})$, represent constraints on the location of the eigenvalues, $\underline{\lambda}$, of the closed loop system in the complex plane. One desirable feature of this formulation is that not all the design specifications have to be incorporated into a single cost function. Constraints, such as damping ratio, bandwidth, etc., that can be more naturally represented as regions in the complex plane can be represented in this way. Others, such as input rate, minimum energy control, etc., can be incorporated into the cost function.

The problem (1)-(5) looks computationally difficult to solve; however, it can be reformulated as follows:

$$\min_{\underline{k} \in S} J = \tfrac{1}{2}\,\mathrm{tr}\{M(\underline{k})P\} \qquad (6)$$

subject to

$$g_i(\underline{\lambda}) \le 0 \qquad i = 1, \ldots, N \qquad (7)$$

where

$$S = \{\underline{k} / (A - BKC) \text{ is asymptotically stable}\} \qquad (8)$$

$$M(\underline{k}) = Q + C^T K^T R K C \qquad (9)$$

$$\tilde{A}(\underline{k}) = A - BKC \qquad (10)$$

$$X_o = E\{\underline{x}(0)\underline{x}^T(0)\} \qquad (11)$$

$$\tilde{A}(\underline{k})P + P\tilde{A}^T(\underline{k}) = -X_o. \qquad (12)$$

Here P is a constant positive definite matrix; $\underline{k}$ is a vector comprised of the elements of the matrix K; $\underline{x}(0)$ is the initial state of the system; and $\tilde{A}(\underline{k})$ is the closed loop system for a given $\underline{k}$. Given this formulation, the cost J is easily found. To solve for J directly from (1), one would first have to calculate $\underline{x}(t)$ for each $\underline{k}$; whereas to solve (6), one has to solve the Lyapunov equation (12) for each $\underline{k}$ and then perform a few simple matrix operations.

The derivation of (6)-(12) from (1)-(5) is standard [13] but included for completeness.

Substitute (3) in (4) and (4) in (1):

$$J = \tfrac{1}{2} E\{\int^{\infty} [x^T Qx + (-KCx)^T R(-KCx)]dt\}$$

$$= \tfrac{1}{2} E\{\int^{\infty} x^T [Q + C^T K^T RKC] x dt\}. \qquad (13)$$

Define $M(\underline{k})$ by equation (9)

$$J = \tfrac{1}{2} \{\int_0^{\infty} x^T Mx dt\}$$

$$= tr\{\tfrac{1}{2} E\{\int_0^{\infty} x^T Mx dt\}\}$$

$$= \tfrac{1}{2} \int_0^{\infty} E\{tr\{x^T Mx\}\}dt$$

$$= \tfrac{1}{2} \int_0^{\infty} E\{tr\{Mxx^T\}\}dt$$

$$= \tfrac{1}{2} tr\{\int_0^{\infty} E\{Mxx^T\}dt\}$$

$$= \tfrac{1}{2} tr\{M\int_0^{\infty} E\{xx^T\}dt\}. \qquad (14)$$

The second equality follows because the trace of a scalar is just equal to the scalar; the third follows due to the commutativity of the trace, integration, and expectation operators, as does the fifth; the fourth is a property of the trace operator; and the sixth is because M is independent of both t and x(t). Now define P as follows and rewrite (14)

$$P \triangleq \int_0^{\infty} E\{xx^T\}dt \qquad (15)$$

$$J = \tfrac{1}{2} tr\{M(\underline{k})P\} \qquad (16)$$

which is of the form of J in equation (6). Moreover, since

$$\underline{x}(t) = e^{\tilde{A}t}\underline{x}(0) \tag{17}$$

where $\tilde{A}$ is the closed loop matrix (10),

$$\begin{aligned} P &= \int_0^\infty E\{e^{\tilde{A}t}x(0)x^T(0)e^{\tilde{A}^T t}\}dt \\ &= \int_0^\infty e^{\tilde{A}t}E\{x(0)x^T(0)\}e^{\tilde{A}^T t}dt. \end{aligned} \tag{18}$$

The second equality follows since the state transition matrix, $e^{\tilde{A}t}$, is independent of the initial state of the system. Finally, for stable $\tilde{A}$, P is the positive definite matrix which satisfies [14]

$$\tilde{A}(\underline{k})P + P\tilde{A}^T(\underline{k}) = -X_o. \tag{19}$$

Thus the reformulated problem (6)-(12) is indeed equivalent to the original problem (1)-(5).

Problem (6)-(12) is a mathematical representation of the problem (described in the introduction of this thesis) of choosing constant output feedback gains for a linear time invariant system subject to certain design criteria which are represented by a cost function and constraints on the locations of eigenvalues in the complex plane. The question of how to solve the problem (6)-(12) remains. Problem (6)-(12) is a nonlinear constrained minimization over a finite dimensional space. The next section will discuss methods of solving such a problem.

3. NONLINEAR PROGRAMMING SOLUTION PROCEDURE

There are several ways to solve a nonlinear problem of the form (6)-(12). As stated previously, the basic problem is

$$\min_{\underline{k}\in S} J(\underline{k}) \tag{20}$$

subject to

$$g_i(\underline{k}) \leq 0 \qquad i = 1,\ldots,N \tag{21}$$

where the exact form of the cost function is defined explicitly by equations (6), (11), and (12) in Section 2 of this thesis. Two of the most common methods of solving a problem of this type are penalty function and Lagrange multiplier methods [15]. Each of these methods has certain problems (to be described below) which are inherent to the method. However, by using a combination of both methods, these problems can be avoided and a better approximation to the solution for (20)-(21) can be obtained [16].

In its simplest form the Lagrange multiplier method solves the following problem [15]

$$\max \varphi(\underline{d}) \tag{22}$$

subject to

$$d_i \geq 0 \qquad i = 1,\ldots,N \tag{23}$$

where $\underline{d} \in R^N$ and

$$\varphi(\underline{d}) = \min_{\underline{k}\in S} J(\underline{k}) + \sum_{i=1}^{N} d_i g_i(\underline{k}). \tag{24}$$

This problem is often easier to solve since the nonlinear constraints, $g_i(\underline{k})$, have been replaced by simple linear ones. The problem (22)-(23) is the dual problem of problem (20)-(21). The duality theorem states that as long as $\varphi(\underline{d}) > -\infty$ for some positive d_i's and $J(\underline{k}) < \infty$ for some $\underline{k}\in S$, the solution to

(22)-(23) is less than or equal to the solution to (20)-(21). When the solution to (22)-(23) is strictly less than the solution to (20)-(21), a duality gap exists [15]. For convex functions with convex constraints, this difficulty does not occur. The solution to (22)-(23) is also the solution for (20)-(21). However, for a general function, $J(\underline{k})$, a duality gap may exist so that the solution to (22)-(23) is a lower bound on the solution to (20)-(21), rather than the time minimum [15].

On the other hand, exterior penalty functions solve the problem [25]:

$$\min_{\underline{k} \in S_1} J(\underline{k}) + cH(\underline{k}) \tag{25}$$

where c is some positive constant, S_1 is the region in R^m where all the constraints, (21), are satisfied, and $H(\underline{k})$ is a functional with these properties:

$$H(\underline{k}) \geq 0 \text{ for all } \underline{k} \in R^m \tag{26}$$

$$H(\underline{k}) \text{ is continuous} \tag{27}$$

$$H(\underline{k}) = 0 \iff \underline{k} \in S_1. \tag{28}$$

As long as $\underline{k} \in S_1$, $H(\underline{k}) = 0$, so problems (20)-(21) and (25) are identical. When $\underline{k}$ is outside S_1, the function $J(\underline{k}) + cH(\underline{k})$ is large. As c becomes large, the minimum of $J(\underline{k}) + cH(\underline{k})$ approaches S_1. The most common penalty function is

$$H(\underline{k}) = \sum_{i=1}^{N} \max[0, g_i(\underline{k})]^2. \tag{29}$$

For this function, the value of $H(\underline{k})$ is the sum of the squares of the distances by which each constraint is violated, so the penalty term increases rapidly when the distance $\underline{k}$ is outside S_1. The advantage of this method is that problem (25) is an unconstrained minimization problem which is often easier to solve than problem (20)-(21). The disadvantage of this approach is that to obtain a good approximation to problem (20)-(21), c must become large. However, as c approaches infinity, the matrix of second partial derivatives of $J(\underline{k}) + cH(\underline{k})$ (the Hessian) becomes increasingly ill conditioned. Many algorithms for unconstrained minimization depend on either the Hessian or an approximation of the Hessian to find the minimum. If the Hessian is ill-conditioned, these algorithms will converge very slowly [15].

By combining penalty function methods with Lagrange multiplier methods, one can eliminate the duality gap and use a smaller value of c, thus improving the conditioning of the Hessian at the solution [17]. Using the penalty function $H(\underline{k})$, in (29), consider the problem:

$$\min_{\underline{k}\in S} J(\underline{k}) + cH(\underline{k}) \tag{30}$$

subject to

$$g_i(\underline{k}) \leq 0 \qquad i = 1,\ldots,N. \tag{31}$$

Given the properties of $H(\underline{k})$, problem (30)-(31) is equivalent to (20)-(21). The dual of problem (30)-(31) is

$$\max g_c(\underline{d}) \tag{32}$$

subject to

$$d_i \geq 0 \qquad i = 1,\ldots,N \tag{33}$$

where

$$g_c(\underline{d}) = \inf_{\underline{k}\in S}\{J(\underline{k}) + cH(\underline{k}) + \sum_{i=1}^{N} d_i g_i(\underline{k})\}. \tag{34}$$

<u>Theorem 1</u>: There exists a $c \in R$ with $0 < c < \infty$ such that the solution to problem (32)-(33) is also the solution to problem (30)-(31).

<u>Proof</u>: See Bertsekas [18].

Theorem 1 implies there is no duality gap for problems (30)-(31) and (32)-(33). Moreover, since the value of c needed to solve this problem exactly is finite, the structure of the Hessian is more favorable for solving the problem.

Bertsekas [19] discusses a variation of problems (30)-(31) and (32)-(33) and suggests a very straightforward way to solve the maximization over $\underline{d}$. He suggests solving the problem

$$\max g_c(\underline{d}) \tag{35}$$

subject to

$$d_i \geq 0 \qquad i = 1,\ldots,N \tag{36}$$

where

$$g_c(\underline{d},\underline{k}) = \inf_{\underline{k}\in S}\{J(\underline{k}) + \frac{1}{2c'} \sum_{i=1}^{N} \{\max[0, d_i + c' g_i(\underline{k})]\}^2 - d_i^2]\}. \tag{37}$$

For the case where the ith constraint is violated, the corresponding term in the summation is

$$d_i g_i(\underline{k}) + c'/2 \; g_i^2(\underline{k}) \tag{38}$$

which is identical to the corresponding term in (34) for $c = c'/2$ and $H(\underline{k})$ as defined in (29). For the case where the ith constraint is satisfied, but

$$d_i + c' g_i(\underline{k}) > 0 \tag{39}$$

equation (38) also applies; and, when

$$d_i + c' g_i(\underline{k}) < 0 \tag{40}$$

the corresponding term in the summation is

$$- \frac{1}{2c'} d_i^2. \tag{41}$$

Bertsekas has shown that the solution to (35)-(36) is equivalent to that of problem (20)-(21) for all values of c' greater than some lower bound $\hat{c}$ ($\hat{c}$ exists and is finite).

One can solve the problem (35)-(36) iteratively, viewing the iteration over $\underline{d}$ as a fixed stepsize gradient problem [19]. The partial of $g_c(\underline{d},\underline{k})$ with respect to d_i is

$$\frac{\partial g_c(\underline{d},\underline{k})}{\partial d_i} = \max[-d_i/c', \ g_i(\underline{k})] \qquad i=1,\ldots,N. \tag{42}$$

Hence the gradient of $g_c(\underline{d},\underline{k})$ with respect to $\underline{d}$ is the vector of these partials. The appropriate update of $\underline{d}_{J+1}$ is

$$\underline{d}_{J+1} = \underline{d}_J + c'\nabla g_c(\underline{d},\underline{k}). \tag{43}$$

For $J(\underline{k})$ and $g_i(\underline{k})$ convex, Bertsekas has shown that his method has demonstrated global convergence for a wide range of step sizes. The main advantages of using this method is that it combines the advantages of both penalty function and Lagrange multiplier methods and that the iterative method to solve the maximization over $\underline{d}$ is very simple.

There remains the problem of solving the minimization over $\underline{k}$ for a fixed $\underline{d}$. This problem can be solved using a variable metric algorithm.[1] At each iteration of the routine the user must supply the value of the function to be minimized and its gradient. From this information, the routine builds up an approximation to the inverse Hessian which improves as the routine gathers information from more points [20].

---

[1] Such as MINOPC of the M.I.T. LID's software library programmed by J. Carrig.

To solve for $g_c(\underline{d},\underline{k})$ in (37) at each iteration, one must solve for $J(\underline{k})$ and $g_i(\underline{k})$, $i = 1,\ldots,N$. For problem (6)-(12) from Section 2, $J(\underline{k})$ can be solved using (6) and (12). The constraints $g_i(\underline{\lambda}(\underline{k}))$ are chosen by the designer and thus are also readily available. The gradients are also needed at each iteration. Taking the partials of $g_c(\underline{d},\underline{k})$ in (37) with respect to $\underline{k}$,

$$\frac{\partial g_c(\underline{d},\underline{k})}{\partial k_i} = \frac{\partial J(\underline{k})}{\partial k_i} + \max[0,\ d_i + c/g_i(\underline{k})]\ \frac{\partial g_i(\underline{k})}{\partial k_i} \ . \tag{44}$$

Thus to solve problem (34), the gradient of the constraints and of the cost with respect to $\underline{k}$ must be provided. Section 4 discusses the computations required to solve for $\nabla_{\underline{k}} J(\underline{k})$ and $\nabla_k g(\underline{k})$.

4. COST AND CONSTRAINT GRADIENT CALCULATIONS

As described in Section 3 our approach to the solution of problem (6)-(12) is to solve the equivalent problem (35)-(37) iteratively. To solve the minimization over $\underline{k}$, for a fixed $\underline{d}$, the gradient of $J(\underline{k})$ with respect to $\underline{k}$ and the gradient of $g_i(\underline{\lambda}(\underline{k}))$ with respect to $\underline{k}$ must be computed. Using linear operator theory, one can derive a fairly simple expression for the gradient of $J(\underline{k})$. Using eigenvalue sensitivity theory, one can derive an expression for the gradients of the constraints with respect to $\underline{k}$ [22].

The gradient of $J(\underline{k})$ with respect to K is as follows:

<u>Theorem 2</u>: $$\nabla_K J(\underline{k}) = (RKCP-B^T\Sigma P)C^T$$

where P and Σ are solutions of

$$\begin{aligned}\tilde{A}^T\Sigma + \Sigma\tilde{A} + M(\underline{k}) &= 0\\ \tilde{A}P + P\tilde{A}^T + X_o &= 0\end{aligned} \tag{45}$$

and A and $M(\underline{k})$ are defined in (10) and (9) respectively.

<u>Proof</u>: See [13].

$\nabla_{\underline{k}} J(\underline{k})$ is found by rearranging $\nabla_K J(\underline{k})$ ($\underline{k}$ is a vector of the elements of the matrix K).

To compute the gradient of the constraints with respect to $\underline{k}$, one must compute the gradient of the eigenvalues with respect to $\underline{k}$. After finding the latter, one can use the rules of implicit differentiation to find the former. Consider equation (46).

$$\underline{w}^T(\tilde{A}-\lambda I)\underline{v} = 0 \tag{46}$$

where $\underline{w}^T$ is the left eigenvector of $\tilde{A}$ and $\underline{v}$ is the right eigenvector corresponding to eigenvalue λ. Since $\underline{w}^T$ and $\underline{v}$ are the eigenvectors of $\tilde{A}$, (46) is true. When the Frechet differential of a function $F(\underline{k})$ exists, it is given by [13]:

$$\delta F(\underline{k},\Delta\underline{k}) \stackrel{\Delta}{=} \frac{\partial}{\partial\varepsilon} F(\underline{k}+\varepsilon\Delta\underline{k})\Big|_{\varepsilon=0}. \tag{47}$$

The Frechet differential (47) can also be written in terms of an inner product as

$$\delta F(\underline{k},\Delta\underline{k}) \stackrel{\Delta}{=} \langle\nabla F(\underline{k}),\Delta\underline{k}\rangle \tag{48}$$

where

$$\langle\nabla F(\underline{k}),\Delta\underline{k}\rangle = \mathrm{tr}\{\nabla F^T(\underline{k})\Delta\underline{k}\}. \tag{49}$$

Take the Frechet differential of both sides of (46)

$$\delta\underline{w}^T(\tilde{A}-\lambda I)\underline{v} + \underline{w}^T(\tilde{A}-\lambda I)\delta\underline{v} + \underline{w}^T(\delta\tilde{A}-\delta\lambda I)\underline{v} = 0. \tag{50}$$

Again since $\underline{w}^T$ and $\underline{v}$ are eigenvectors, the first two terms are identically zero, thus

$$\underline{w}^T\delta\lambda\underline{v} = \underline{w}^T\delta\tilde{A}\underline{v}. \tag{51}$$

Since $\delta\lambda$ is a scalar,

$$\delta\lambda\underline{w}^T\underline{v} = \underline{w}^T\delta\tilde{A}\underline{v}. \tag{52}$$

Since $\underline{w}^T\underline{v}$ is also scalar

$$\delta\lambda = \frac{\underline{w}^T\delta\tilde{A}\underline{v}}{\underline{w}^T\underline{v}}. \tag{53}$$

Notice, however, that if $\underline{w}^T\underline{v}=0$, equation (53) will not hold. If $\underline{w}^T\underline{v}=0$, then the left eigenvector, $\underline{w}^T$, is perpendicular to the right eigenvector, $\underline{v}$. This only happens when $\tilde{A}$ has a Jordan block of dimension greater than one.

Continuing, from definition (10) and (48)

$$\begin{aligned}\delta\tilde{A}(K,\Delta K) &= \frac{\partial}{\partial\varepsilon}\tilde{A}(K+\varepsilon\Delta K)\Big|_{\varepsilon=0}\\ &= \frac{\partial}{\partial\varepsilon}[A-B(K+\varepsilon\Delta K)C]\Big|_{\varepsilon=0}\\ &= -B\Delta KC.\end{aligned} \tag{54}$$

Using definition (48).

$$\delta\lambda(K,\Delta K) = \langle \nabla\lambda(K), \Delta K\rangle$$
$$= tr\{\nabla\lambda^T(K)\Delta K\}. \qquad (55)$$

Substituting (54) and (55) in (53):

$$tr\{\nabla\lambda^T(K)\Delta K\} = \frac{\underline{w}^T(-B\Delta KC)\underline{v}}{\underline{w}^T\underline{v}}$$
$$= tr\{-\frac{\underline{w}^T(B\Delta K)C\underline{v}}{\underline{w}^T\underline{v}}\}$$
$$= tr\{-[\frac{C\underline{v}\,\underline{w}^TB}{\underline{w}^T\underline{v}}]\,\Delta K\}. \qquad (56)$$

Since (56) must hold for an arbitrary ΔK,

$$\nabla\lambda^T(K) = -\left[\frac{C\underline{v}\,\underline{w}^TB}{\underline{w}^T\underline{v}}\right] \qquad (57)$$

or

$$\nabla\underline{\lambda}(K) = -\frac{B^T\underline{w}\,\underline{v}^TC^T}{\underline{w}^T\underline{v}}\ . \qquad (58)$$

$\nabla_{\underline{k}}\underline{\lambda}(\underline{k})$ is found by rearranging $\nabla_K\underline{\lambda}(K)$ ($\underline{k}$ is a vector comprised of the elements of K).

Define λ_i in terms of two real variables, σ_i and ω_i.

$$\lambda_i = \sigma_i + j\omega_i. \qquad (59)$$

Then

$$\frac{\partial\sigma_i}{\partial k_i} = \mathrm{Real}(\frac{\partial\lambda_i}{\partial k_i}) \qquad (60)$$

$$\frac{\partial\omega_i}{\partial k_i} = \mathrm{Imaginary}(\frac{\partial\lambda_i}{\partial k_i}). \qquad (61)$$

The constraint functions $g_i(\lambda)$ from equation (7) are considered functions of the two real variables, σ and ω. For the purposes of problem (6)-(12) each constraint will be a function of only one eigenvalue. If all the eigenvalues must lie inside a particular boundary, then n of the constraints will be the equation for the boundary (one for each eigenvalue). Given this situation,

$$\left(\frac{\partial g_i(\sigma_j,\omega_j)}{\partial \underline{k}}\right) = \left(\frac{\partial g_i(\sigma_j,\omega_j)}{\partial \sigma_j}\right)\left(\frac{\partial \sigma_j}{\partial \underline{k}}\right) + \left(\frac{\partial g_i(\sigma_j,\omega_j)}{\partial \omega_j}\right)\left(\frac{\partial \omega_j}{\partial \underline{k}}\right) . \qquad (62)$$

Since the regions in the complex plane are chosen by the designer, it will be assumed that the regions are chosen so that the partials with respect to σ and ω exist. For the same reason, the functions $g_i(\sigma,\omega)$ are known explicitly, and thus, so are the partials. Thus using equations (58)-(62), the gradient of the constraints with respect to the feedback gains, $\underline{k}$, can be calculated.

In summary, both the gradients of the constraints with respect to $\underline{k}$ and the gradient of the cost $J(\underline{k})$, as well as the values of the constraints and the cost, can be calculated given a point $\underline{k}$. Using this information, one can find the solution to (6)-(12) by solving the equivalent problem (32)-(34) as described in Section 3. The next section will discuss some of the specific details and problems involved in implementing this method to solve the reformulated problem (6)-(12).

5. SECOND ORDER EXAMPLE

The purpose of the numerical example of this section is to demonstrate how well the method developed in Section 2 to solve problem (1)-(6) works on a simple second order example. The problem is as follows:

$$\min_{\underline{k} \in S} J = \tfrac{1}{2} \int_0^\infty u^T(t) u(t)\, dt \tag{63}$$

subject to

$$\dot{\underline{x}}(t) = A\underline{x}(t) + B\underline{u}(t) \tag{64}$$

$$u(t) = -[k_1 \quad k_2]\underline{x}(t) \tag{65}$$

$$S = \{\underline{k}/(A-B\underline{k}) \text{ is asymptotically stable}\} \tag{66}$$

$$A = \begin{bmatrix} -1 & 5 \\ -5 & -1 \end{bmatrix} \qquad B = \begin{bmatrix} 0 \\ 1 \end{bmatrix} \tag{67}$$

$$g_i(\sigma,\omega) \leq 0 \qquad i = 1,4 \tag{68}$$

where σ and ω are the real and imaginary parts of the eigenvalues of the closed loop system. The constraints are (see Figure 1):

$$g_1(\sigma,\omega) = \omega - 2.6\sigma \tag{69}$$

$$g_2(\sigma,\omega) = \omega + 2.6\sigma \tag{70}$$

$$g_3(\sigma,\omega) = 4.0804 - \sigma^2 - \omega^2 \tag{71}$$

$$g_4(\sigma,\omega) = \sigma^2 + \omega^2 - 53.1441. \tag{72}$$

Each of these four equations must be satisfied for both eigenvalues so there are actually eight constraints.

Examining a second order system with a single input is particularly convenient for demonstrating the behavior of this algorithm. First, for a second order system one can derive explicit equations relating the feedback

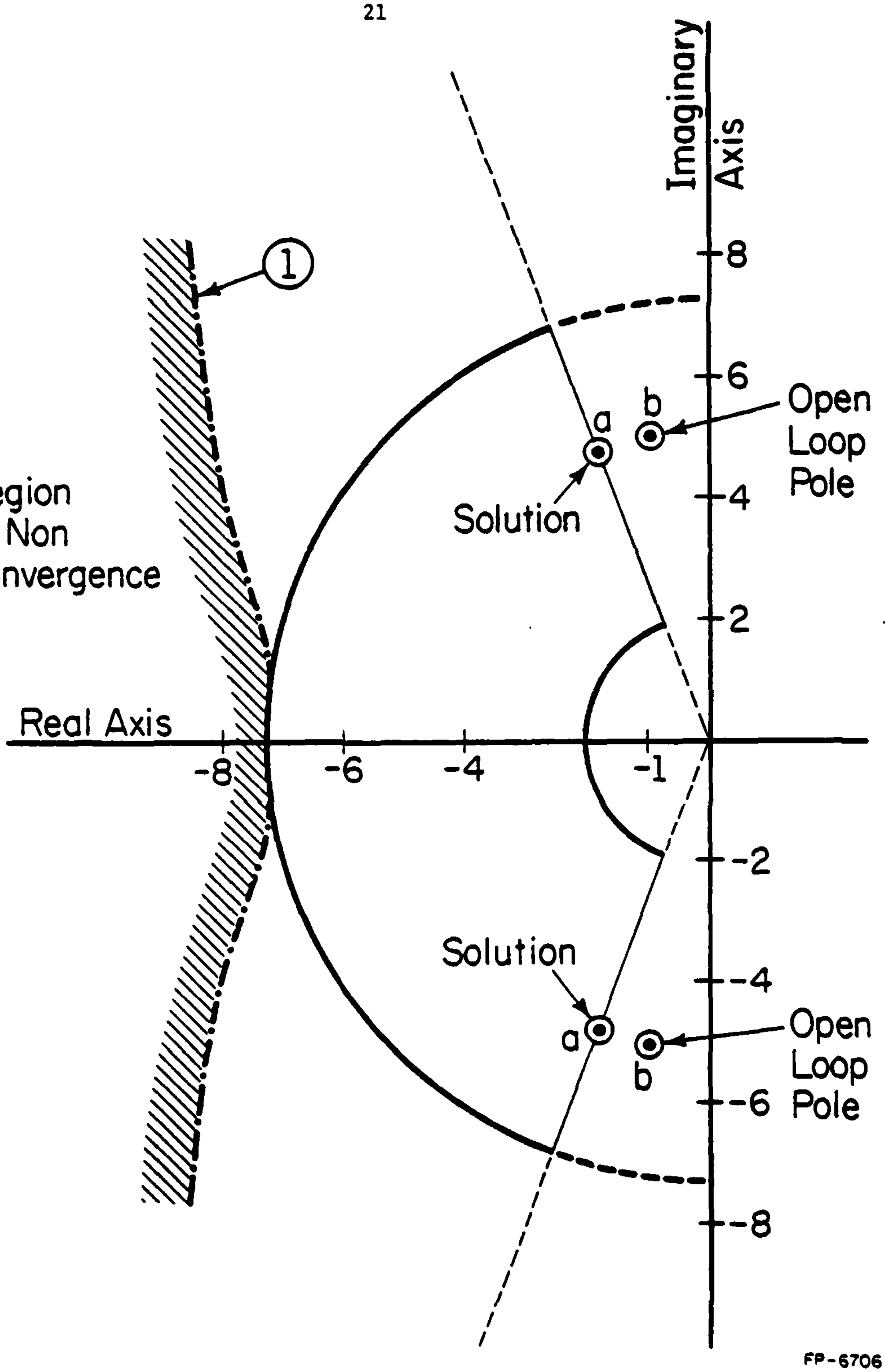

Figure 1. Second order example: constraint region in the complex plane.

gains to the eigenvalues of the closed loop system. Second, equations mapping the boundaries in the complex plane to boundaries in k-space (the space of feedback gains) can be obtained using the mapping method described in [1]. For this second order system and reasonable boundaries, like those given in (69)-(72), the boundaries in k-space are not too complex (Figure 2). Since the minimization is actually over $\underline{k}$ in the k-plane, Figure 2 shows exactly what the constraints are in this space.

The closed loop characteristic equation for this system is

$$\lambda^2 + (2+k_2)\lambda + (26+5k_1+k_2) = 0. \tag{73}$$

Applying the quadratic formula to (73) yields

$$\lambda_1,\lambda_2 = -(1+.5k_2) \pm .5(k_2^2 - 20k_1 - 100)^{1/2}. \tag{74}$$

Taking the partials of λ_1 and λ_2 with respect to k_1 and k_2,

$$\frac{\partial\lambda_{1,2}}{\partial k_1} = \mp 10(k_2^2 - 20k_1 - 100)^{-1/2} \tag{75}$$

$$\frac{\partial\lambda_{1,2}}{\partial k_2} = -.5 \pm .5k_2(k_2^2 - 20k_1 - 100)^{-1/2}. \tag{76}$$

From (75) and (76), one can see that these partials have discontinuities precisely at the boundary where the closed loop system poles change from a complex pair to two real poles or vice versa. Not only are these partials discontinuous at this boundary, their magnitude approaches infinity as the poles approach this boundary. The equation of this boundary in k-space is

$$k_2^2 - 20k_1 - 100 = 0 \tag{77}$$

which corresponds to boundary 9 in Figure 2.

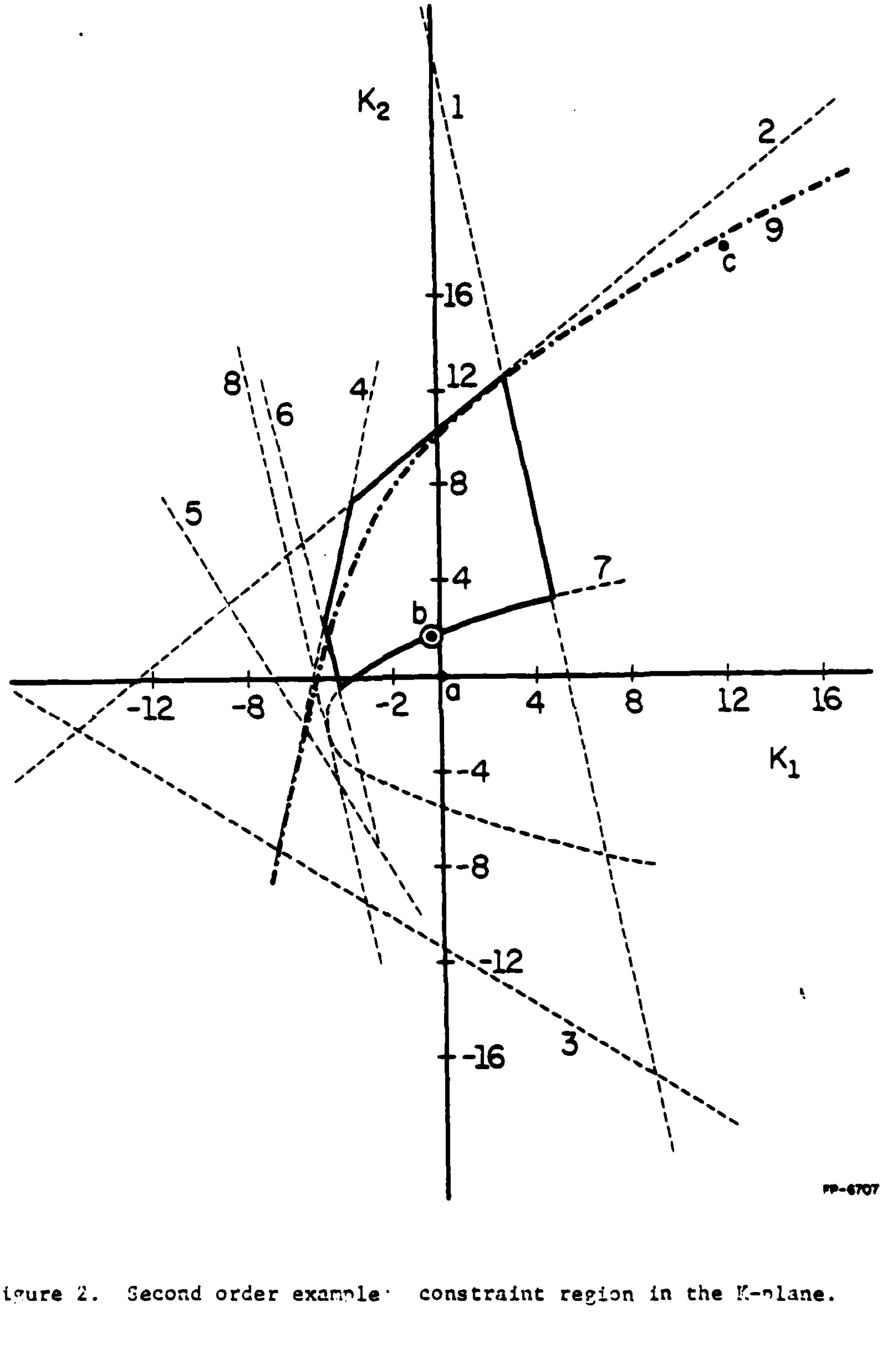

Figure 2. Second order example: constraint region in the K-plane.

The other boundaries in Figure 2 correspond to the boundaries in the complex plane (Figure 1) as follows: the large circle (Figure 1) maps into the triangle formed by 1, 2, and 3 (Figure 2), the small circle maps into the triangle formed by 4, 5, and 6, the two lines into boundaries 7 and 8. The region enclosed by the solid line in Figure 2 is the region in the k-plane where all the constraints (69)-(72) are satisfied. The reason for choosing these boundaries in the complex plane is that such boundaries do occur in real problems (e.g., the aircraft example in the next section) as constraints on the locations of closed loop system poles. A nice feature of using circles for boundaries in the complex plane is that for second order systems circles map into triangles in the k-plane. Hence some of the boundaries in the k-plane are straight lines [21].

The problem (63)-(68) is to find the minimum energy control subject to the indicated constraints. Since system (64) is stable, the minimum energy control without constraints corresponds to zero gain. With the feedback gains set to zero, the poles of (64) are

$$\lambda_1, \lambda_2 = -1 \pm j5. \tag{78}$$

With the given constraints (Figure 1), the minimum energy feedback gains were found to be

$$k = [-.273 \quad +1.68] \tag{79}$$

which places the closed loop poles at

$$\lambda_1, \lambda_2 = -1.84 \pm j4.788. \tag{80}$$

This answer makes sense. From Figure 2, one can see that this point $\underline{k}$ (points b) is approximately the point inside the constraint region closest to the origin. From Figure 1, one can see that the closed loop eigenvalues (points a) are about as close to the open loop eigenvalues (points b) as possible given the constraints. The algorithm converged to the minimum $\underline{k}$ (79) for a wide range of initial guesses for $\underline{k}$. Initial guesses for $\underline{k}$ which placed the closed loop poles outside the large circle and to the left of boundary 1 were the only ones for which the algorithm did not converge to the value of $\underline{k}$ given in (79).

The region in the complex plane for which the algorithm did not converge corresponds to the area in the k-plane (Figure 2) to the right of line 1 and just below curve 9. The fact that the algorithm could not converge from these points can be explained by the discontinuities in the partials of the eigenvalues with respect to $\underline{k}$ mentioned in (75)-(77). Consider point c (Figure 2) as a typical point in this region. It corresponds to a complex pole pair outside the large circle in Figure 1. Line 1 in the k-plane represents the boundary for a complex pole pair crossing this circle; thus, the negative of the gradient in the k-plane for these points points towards line 1 and nearly perpendicular to it. Moving in this direction should reduce the cost function (37). However notice that from point c, for example, movement in this direction will lead to guesses for $\underline{k}$ which fall above or on curve 9. A point on curve 9 corresponds to a double real root for which the partials of the eigenvalues with respect to $\underline{k}$ are infinite. This will obviously cause problems. Notice also that for two real poles, the direction of decreasing cost is determined by boundary 2; whereas, for a complex pair, the direction of decreasing cost is determined by line 1. For all these points - points for which the routine would not converge to (79) - the minimization routine found points which approached boundary 9. However, the algorithm was not able to move across or along the boundary. In summary, the derivatives of the constraints with respect to the feedback gains are not continuous. This fact can lead to convergence problems. However, one can avoid these problems by choosing a better initial guess for $\underline{k}$ (and lower values for c).

This example was also used to study the behavior of the algorithm with respect to changes in the constant c' in (37). As discussed in the section on nonlinear programming, for a very large value of c', the minimization over $\underline{k}$ converges to a solution which is close to the solution to the actual problem, in this case (63)-(68). For a smaller c', each iteration over $\underline{k}$ stops farther from the real solution than with a larger c', but the iterations over $\underline{d}$ lead more quickly to the true solution of the problem. For this problem, c' equal to 2000 seemed to work best. The minimization over $\underline{k}$ led to a solution which was very close to the final solution of the algorithm. The iterations over $\underline{d}$ merely served to bring the point a bit closer to the boundaries (within 10^{-7}, instead of 10^{-3}). This was true even for smaller values of c', 20 and 200. The smaller values of c' led to more iterations over $\underline{d}$, but fewer over $\underline{k}$ at each substep. For c' equal to 2, the first iteration over $\underline{k}$ did converge to a solution which was different from the solution with c' equal to 2000. However the iterations over $\underline{d}$ led to the same final solution as with c' equal to 2000. In terms of total function evaluations, c' equal to 2000 was the most efficient; moreover, the solutions for smaller values of c' were not significantly different from those with c' equal to 2000.

To summarize the results for this example, this algorithm works provided a good initial guess for $\underline{k}$ and a reasonable value of c' are used.

Provided these two conditions are satisfied, the minimum energy feedback gains for problem (63)-(68) are

$$k = [-.273 \quad +1.68]. \tag{81}$$

This gain places the closed loop system poles at

$$\lambda_1, \lambda_2 = -1.84 \pm j4.788. \tag{82}$$

The next two sections will present a more complex example and discuss some results for that example.

6. AIRPLANE EXAMPLE

The system studied in this example is a linearized model of the longitudinal motion of a fighter aircraft. The description of the system model and the design criteria are taken from [12] with minor differences (see below). The solution method in [12] is the parameter mapping technique described in [1]. This thesis will use the nonlinear programming method developed in the previous sections.

The particular aircraft considered in this example is a McDonnell-Douglas F4-E with horizontal canards. A complete description of the F4-E is given in [23]. The behavior of the aircraft was modeled by four sets of system matrices, one for each of four flight conditions (see Tables 1-3). One design objective was to find a set of constant feedback gains which place the closed loop system poles in certain regions of the complex plane (different regions for each flight condition, see Figure 4). The second was to find a set of gains which satisfied the above criteria and also placed the closed loop system poles within certain emergency regions in the case that a sensor failed (Figure 5). The condition of a sensor failure was considered to be equivalent to setting the corresponding feedback gain equal to zero.

Figure 3 shows some of the important quantities for studying the longitudinal motion of the F4-E. For this plane, two dominant modes determine the longitudinal rigid body motion of the plane - the phugoid mode which is very slow and the short period mode which has the most effect on the handling qualities of the plane. Uncontrolled, the short period mode is unstable for all subsonic flight conditions (see Table 2).

Table 1. Physical definition of the four flight conditions

Flight Condition	Mach	Altitude
1	.5	5000'
2	.85	5000'
3	.9	35000'
4	1.5	35000'

Table 2. Open loop eigenvalues

Flight Conditions	Short Period Mode	Phugiod Mode
1	-3.07, +1.23	-14
2	-4.9 , +1.78	-14
3	-1.87, +.56	-14
4	-.87 $\pm j4.3$	-14

Table 3. Aero data for equation (84)

	Flight Condition #1	Flight Condition #2	Flight Condition #3	Flight Condition #4
a_{11}	-.9896	-1.702	-.6607	-.5162
a_{12}	17.41	50.72	18.11	26.96
a_{13}	96.15	263.5	84.34	178.9
a_{21}	.2648	.2201	.08201	-.6896
a_{22}	-.8512	-1.418	-.6587	-1.225
a_{23}	-11.39	-31.99	-10.81	-30.38
b_1	-97.78	-272.2	-85.09	-175.8

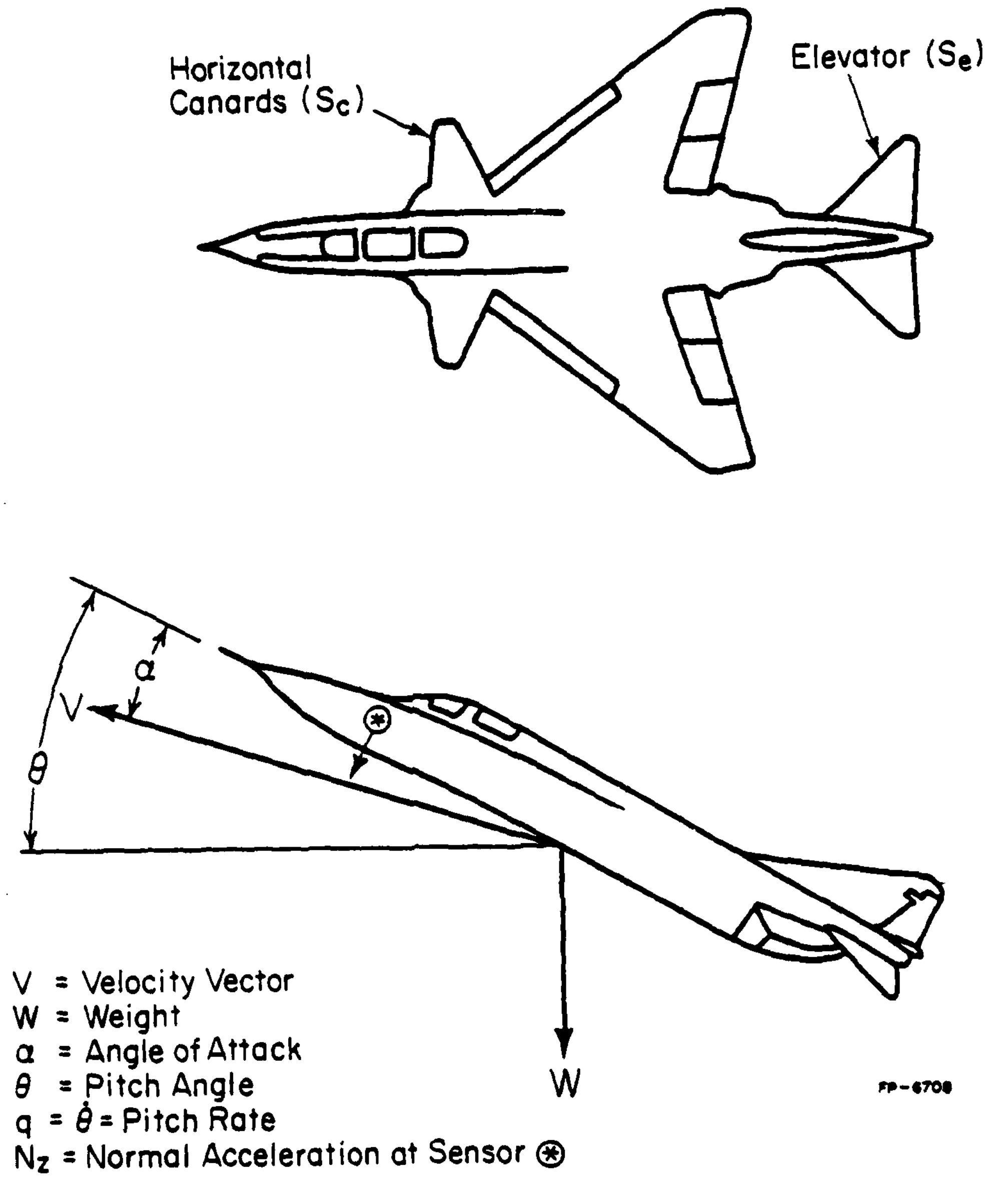

Figure 3. Definition of aircraft variables.

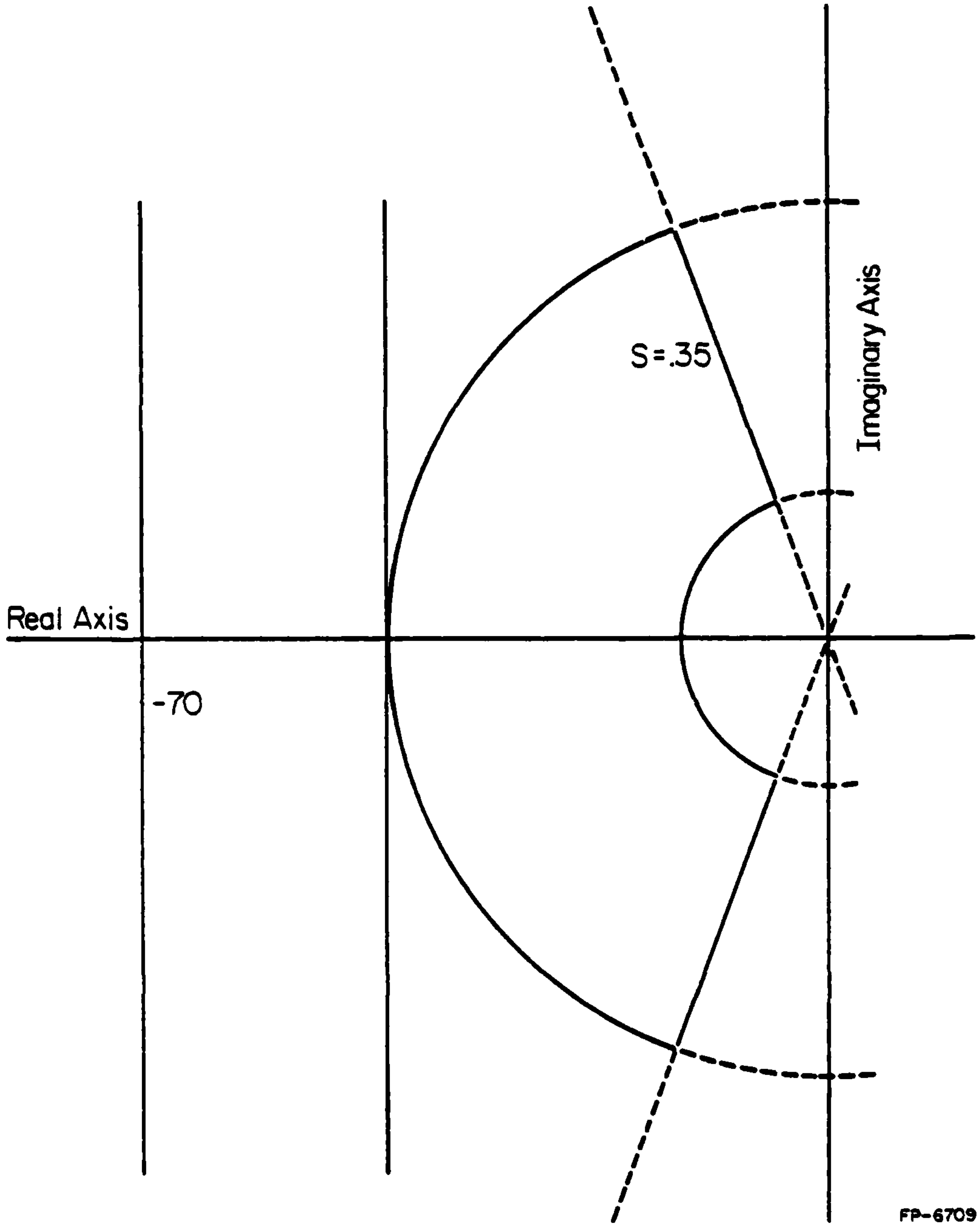

Figure 4. Aircraft example: constraint region in the complex plane under normal operating conditions.

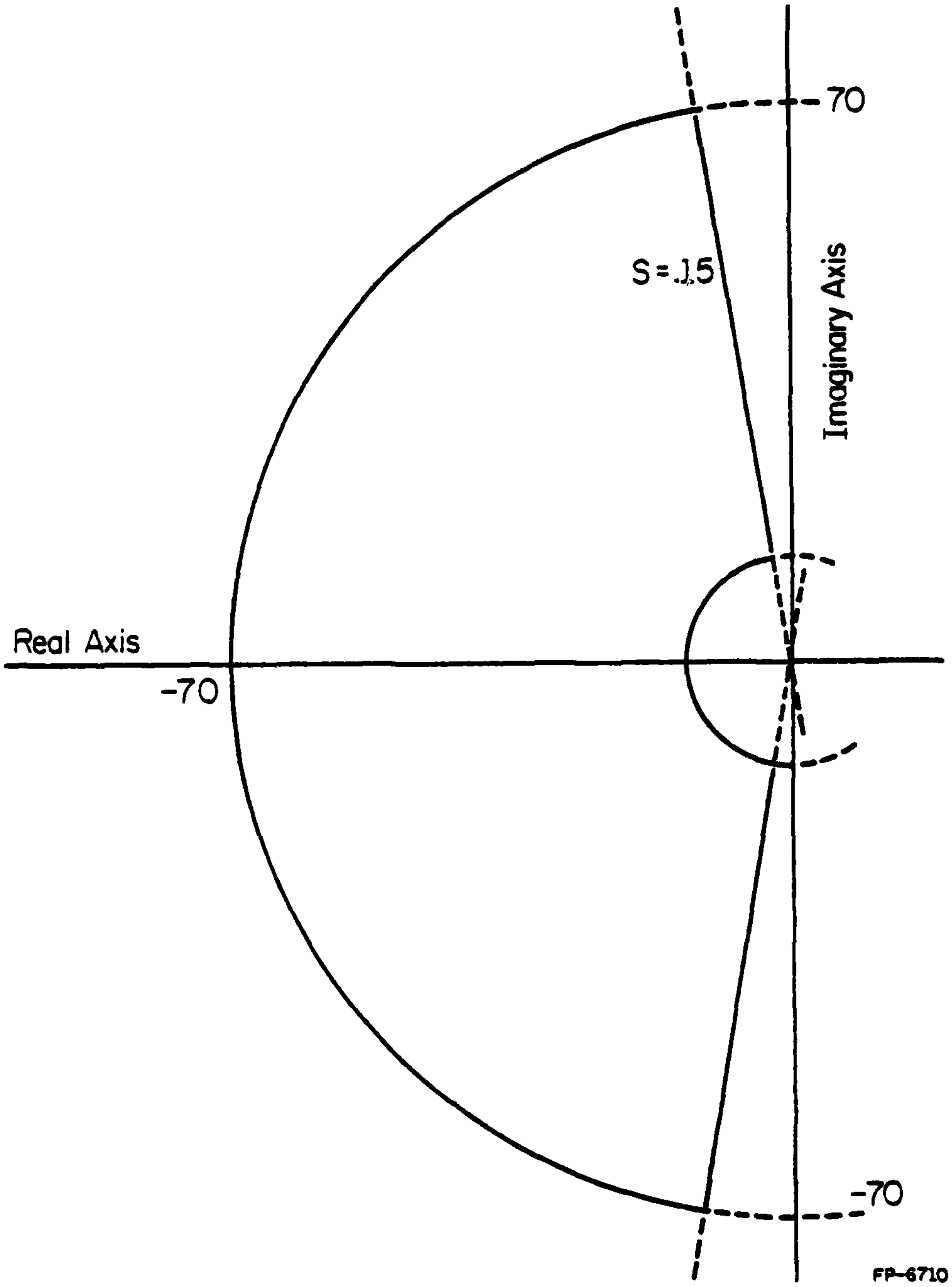

Figure 5. Constraint region in the complex plane: emergency conditions.

The two major control surfaces available for controlling the short period mode are the elevator position, δ_e, and the canard position, δ_c (see Figure 3). The simplified model used for these actuators was

$$\dot{\delta} = -a\delta + a\,\delta_{com} \tag{83}$$

where δ is the actuator position, δ_{com} is the commanded actuator position, and a is the equivalent bandwidth of the actuator which was assumed to be 14 rad/s. Since the canard command was found to be proportional to the elevator command, a state model was derived which incorporated these two quantities into one state δ_e which represents the effective control of the elevator and the canard together.

The other two quantities that are often used to control the pitch axis are the pitch rate (q) and the normal accelerator (N_z) (see Figure 3). These two quantities, as well as δ_e, were assumed to be available for feedback.[1] The following is the system model for this airplane, based on these quantities. For a complete description of the derivation of these equations see [12].

$$\frac{d}{dt}\begin{bmatrix} N_z \\ q \\ \delta_e \end{bmatrix} = \begin{bmatrix} a_{11} & a_{12} & a_{13} \\ a_{21} & a_{22} & a_{23} \\ 0 & 0 & -a \end{bmatrix}\begin{bmatrix} N_z \\ q \\ \delta_e \end{bmatrix} + \begin{bmatrix} b_1 \\ 0 \\ a \end{bmatrix} u \tag{84}$$

$$y(t) = \begin{bmatrix} 1 & 0 & 0 \\ 0 & 1 & 0 \\ 0 & 0 & 1 \end{bmatrix}\begin{bmatrix} N_z \\ q \\ \delta_e \end{bmatrix} \tag{85}$$

$$u(t) = -\underline{k}y(t). \tag{86}$$

---

[1] Franklin [12] used only the first two variables in the feedback design.

As previously stated, a was assumed to be 14 rad/s. The values a_{ij} and b_1 are different for each flight condition and are given in Table 3. The matrix $\underline{k}$ is to be determined.

One design problem for this airplane was to choose $\underline{k}$ such that the closed loop eigenvalues for each flight condition are in certain regions in the complex plane (Figure 4). Ideally one would like to find one set of gains which worked for all four flight conditions. The constraints on the short period eigenvalues are given by restrictions on the damping and the natural frequency of the short period mode. The characteristic equation for these eigenvalues is

$$\lambda^2 + 2\xi_{sp}\omega_{sp}\lambda + \omega_{sp}^2 = 0 \tag{87}$$

where ξ_{sp} is the damping and ω_{sp} is the natural frequency. Under normal operating conditions (i.e., no sensor failures), ξ_{sp} and ω_{sp} are required to satisfy

$$.35 < \xi_{sp} < 1.3 \tag{88}$$

$$\omega_a < \omega_{sp} < \omega_b \tag{89}$$

where ω_a and ω_b depend on the flight condition (see Table 4). For the case when one of the sensors fail, ξ_{sp} and ω_{sp} must satisfy

$$.15 < \xi_{sp} \tag{90}$$

$$\omega_c < \omega_{sp} \tag{91}$$

where ω_c depends on the flight condition (Table 4). For the emergency situation, the actuator pole is also required to satisfy (90)-(91). For the nonemergency situation, the actuator pole (λ_a) is required to satisfy

$$\omega_b < \lambda_a < 70 \text{ rad/s.} \tag{92}$$

These regions in the complex plane are shown in Figures 4 and 5.

For this thesis, an additional design criterion was added. The feedback gains were to be chosen such that the minimum total control energy is used given the constraints on the locations of the closed-loop poles described above. The appropriate cost function to minimize is

$$\min_{k \in S} J = \int_0^\infty u^T(t)u(t)dt \tag{93}$$

where S is the set of feedback gains for which the closed loop system (84)-(86) is asymptotically stable. Taken together with appropriate equations for the constraints in Figures 4 and 5, equations (84)-(86) and (93) represent a problem of the form (1)-(6) in Section 2. Thus the method of solution developed in the previous sections of this thesis can be applied. The results for this example are discussed in the next section.

Table 4. Frequency limits which determine boundaries in Figures 4 and 5

	Flight Condition #1	Flight Condition #2	Flight Condition #3	Flight Condition #4
ω_a (rad/s)	2.02	3.50	2.19	3.29
ω_b (rad/s)	7.23	12.6	7.86	11.8
ω_c (rad/s)	1.53	2.65	1.65	2.49

7. RESULTS AND DISCUSSION FOR AIRPLANE EXAMPLE

The design problem for the F4-E airplane considered by this thesis is to find one set of constant feedback gains for which the closed loop system poles are in the appropriate region in the complex plane for each one of the four flight conditions under normal operating conditions. After finding such a solution, the next problem is to look for a set of gains that satisfies the above criteria and also is robust with respect to sensor failures.

First, each flight condition was studied separately to see if a fixed gain controller could be found to satisfy the constraints under normal operating conditions. As mentioned in Section 5, a good initial guess for the feedback gains is important for the algorithm to converge properly. Since the problem is to find the constrained minimum for J in (93), one sensible starting point is the set of gains which correspond to the unconstrained minimum of J. One can find these gains simply enough by solving a Riccati equation for each set of system matrices [24]. These gains were used, and gains for a fixed gain controller were found for each flight condition. The next step was to find one set of gains which would work for all four flight conditions.

Such a set of gains was found both for the case when all three states (84) were available and for the case when only the first two were available. Franklin [12] considered the latter case. Rather than looking for a particular set of gains, the procedure used in [12] was to map the constraints from the complex plane (Figure 4) into the space of feedback gains. The entire region of possible gains which satisfy the constraints

(Figure 6) was found. Using the method described in this thesis, the minimum energy $\underline{k}$ using only two gains was found to be (see Table 5)

$$\underline{k} = [-2.8281124 \times 10^{-2} \quad -2.0652172 \times 10^{-1}]. \tag{94}$$

This point is marked in Figure 6 and is near the boundary of the enclosed region found by Franklin, at the point approximately nearest the origin. Thus the results presented in this thesis are consistent with Franklin's. For the case with three feedback gains, the minimum energy $\underline{k}$ was found to be (see Table 6)

$$\underline{k} = [-3.8498269 \times 10^{-2} \quad -2.7574095 \times 10^{-1} \quad 3.3295187 \times 10^{-1}] \tag{95}$$

An important measure of system performance is the C_N^* response discussed in [12]. The C_N^* is a linear combination of the normal acceleration and the pitch rate of the plane, given by

$$C_N^* = (N_z + 12.43q)/k_c^* \tag{96}$$

where k_c is the stationary value of C_N^* and is used for normalization. The C_N^* response to a step input should fall in the region shown in Figure 7. Figure 8 shows this response for each of the four flight conditions. The first column consists of the responses for the design presented in this thesis with $\underline{k}$ as given in equation (95). Comparing these responses with Figure 7, one can see that they do lie within the required region. The second column contains the C_N^* responses for the following gain matrix

$$\underline{k} = [-.115 \quad -.8] \tag{97}$$

which is the design used in [12]. These C_N^* time responses appear to be faster and to satisfy the requirement given by Figure 7 better than those presented in this thesis. This is not surprising; the gains (97) were

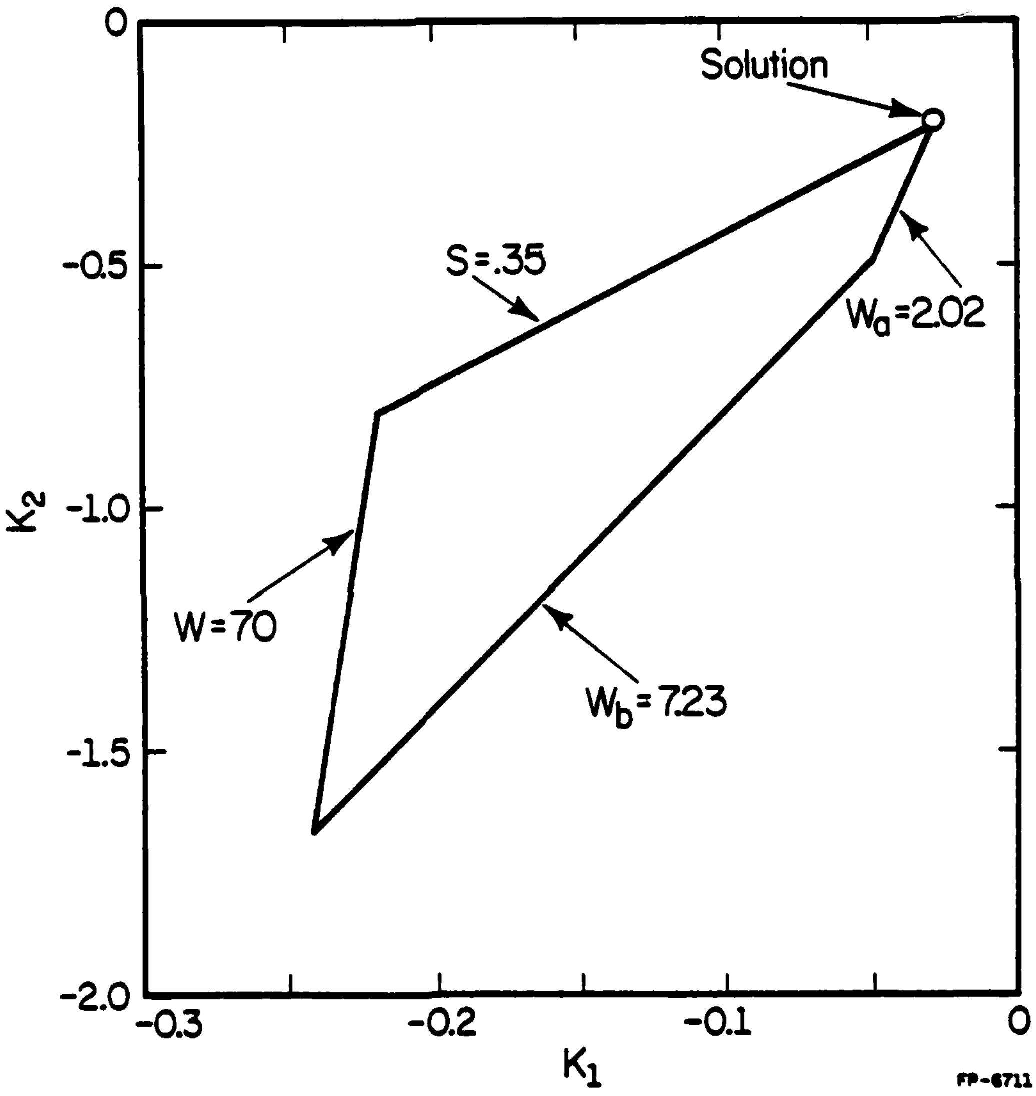

Figure 6. Region of possible gains which satisfy the constraints under normal operating conditions for all four flight conditions.

Table 5. Minimum energy feedback gains: normal operating condition solution (2 gains)

$\underline{k} = [-2.8281124\times10^{-2} \quad -2.0652172\times10^{-1}]$	
Flight Condition #	Closed Loop Eigenvalues
1	-2.0483019, -2.0200008, -14.537826
2	$-3.1624007 \pm j5.2143045$, -18.493321
3	$-1.589176 \pm j1.7992842$, -14.547498
4	$-2.1992634 \pm j5.8851873$, -16.308839

Table 6. Minimum energy feedback gains: normal operating condition solution (3 gains)

$\underline{k} = [-3.8498269\times10^{-2} \quad -2.7574095\times10^{-1} \quad 3.3295187\times10^{-1}]$	
Flight Condition #	Closed Loop Eigenvalues
1	$-2.0194637 \pm j3.3183791\times10^{-9}$, -20.227559
2	$-3.3792113 \pm j5.0261318$, -25.502133
3	$-1.5977817 \pm j1.7690526$, -20.060981
4	$-2.2968881 \pm j5.7580029$, -22.569046

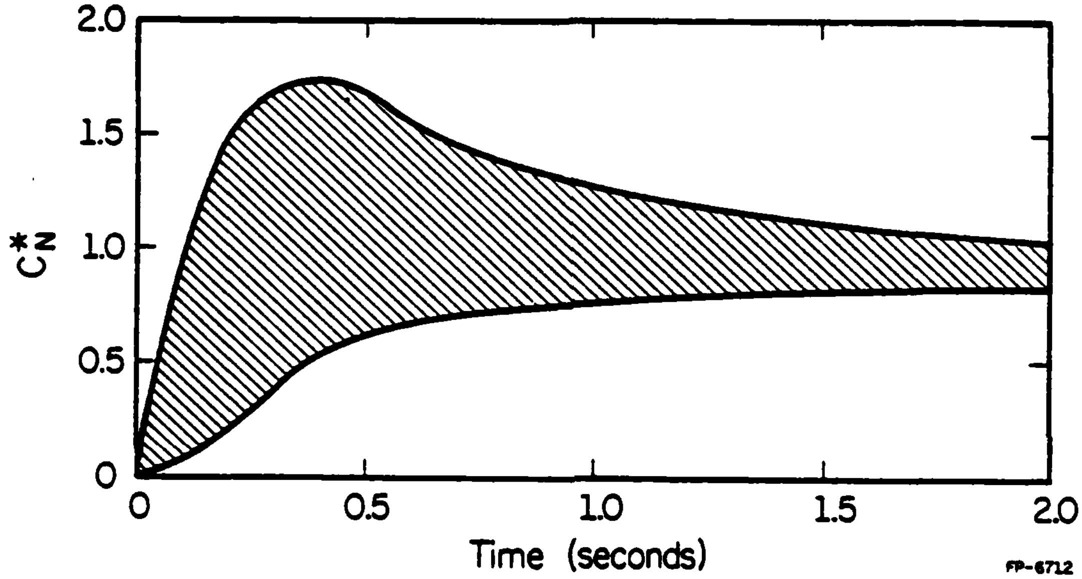

Figure 7. C_N^* response envelope.

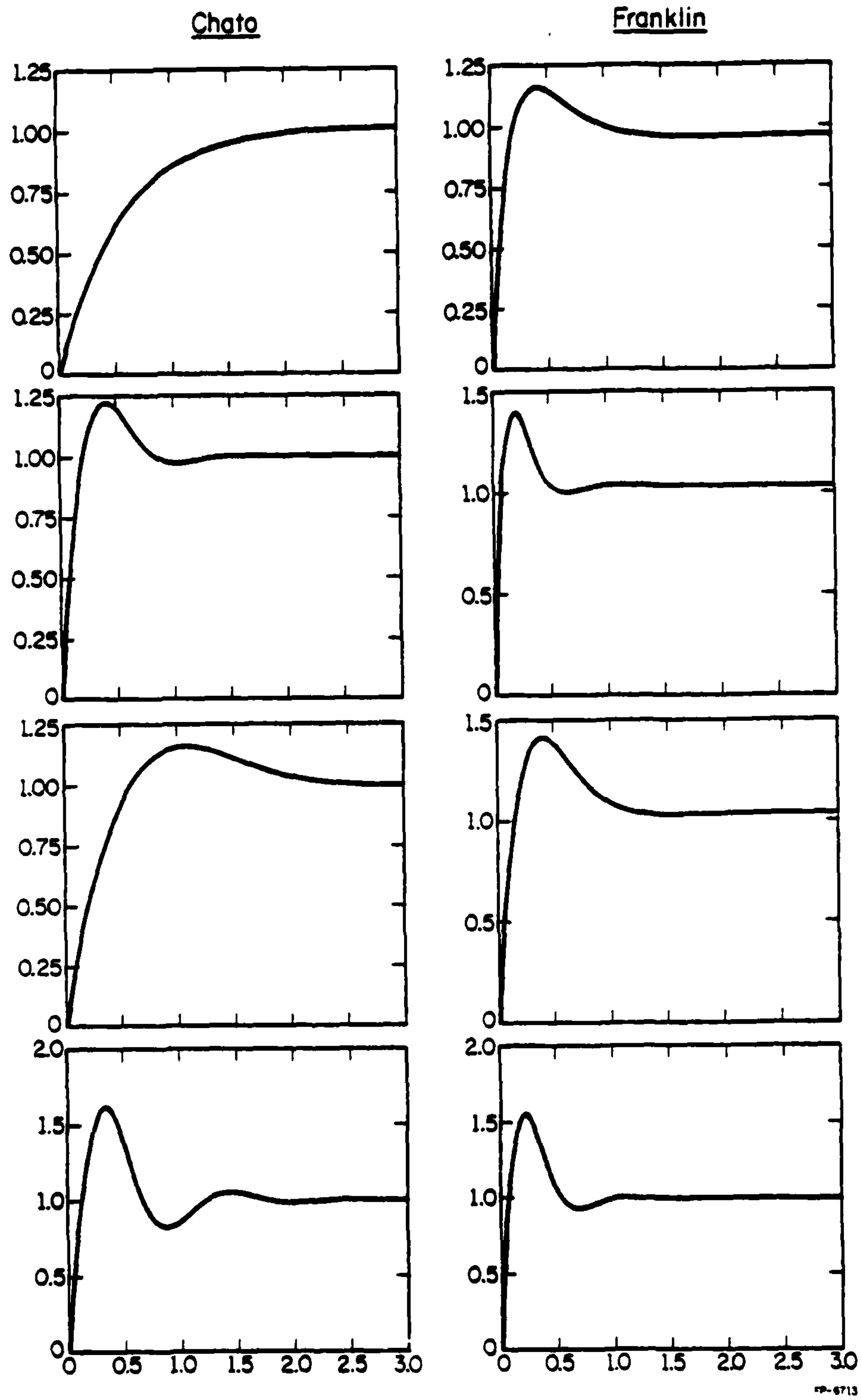

Figure 8. C_N^* responses of two designs.

chosen on the basis of the C_N^* criterion. The criterion used to choose the gains for this thesis was the minimization of the control energy. Thus, slower C_N^* responses should be expected.

More specifically, the design criterion used to choose the gains in equation (95) was the minimization of the control energy required to bring the system back to equilibrium from a disturbance. Figure 9 shows u(t) for each of the four flight conditions (the first column contains the ones for this thesis; the second for those of [12]). From these figures, one can see that the controls for this thesis are considerably smaller than the controls which result from [12]. However, the system is stabilized faster (but at the expense of actuator control) for the gain (97).

Franklin choose his feedback gains (97) by looking at the time responses for several points and picking the best one. For this thesis, the gains (95) were chosen by using a cost function which represented the minimum energy control. By changing the cost function or the constraint boundaries in the complex plane, one could easily incorporate the C_N^* response criterion into the design. One could also choose the cost and the boundaries so that the solution would be a compromise between the minimum energy control and a fast response. Moreover, the results from this design indicate where trade-offs can be made and how to make them. In short, using a cost function to choose a set of feedback gains may provide more insight than trial and error alone.

Franklin [12] also mapped the emergency regions in the complex plane (Figure 5) into the gain space for the case with only two feedback gains. Unfortunately, the region for which all the constraints for both the normal and the emergency situations are satisfied does not intersect either

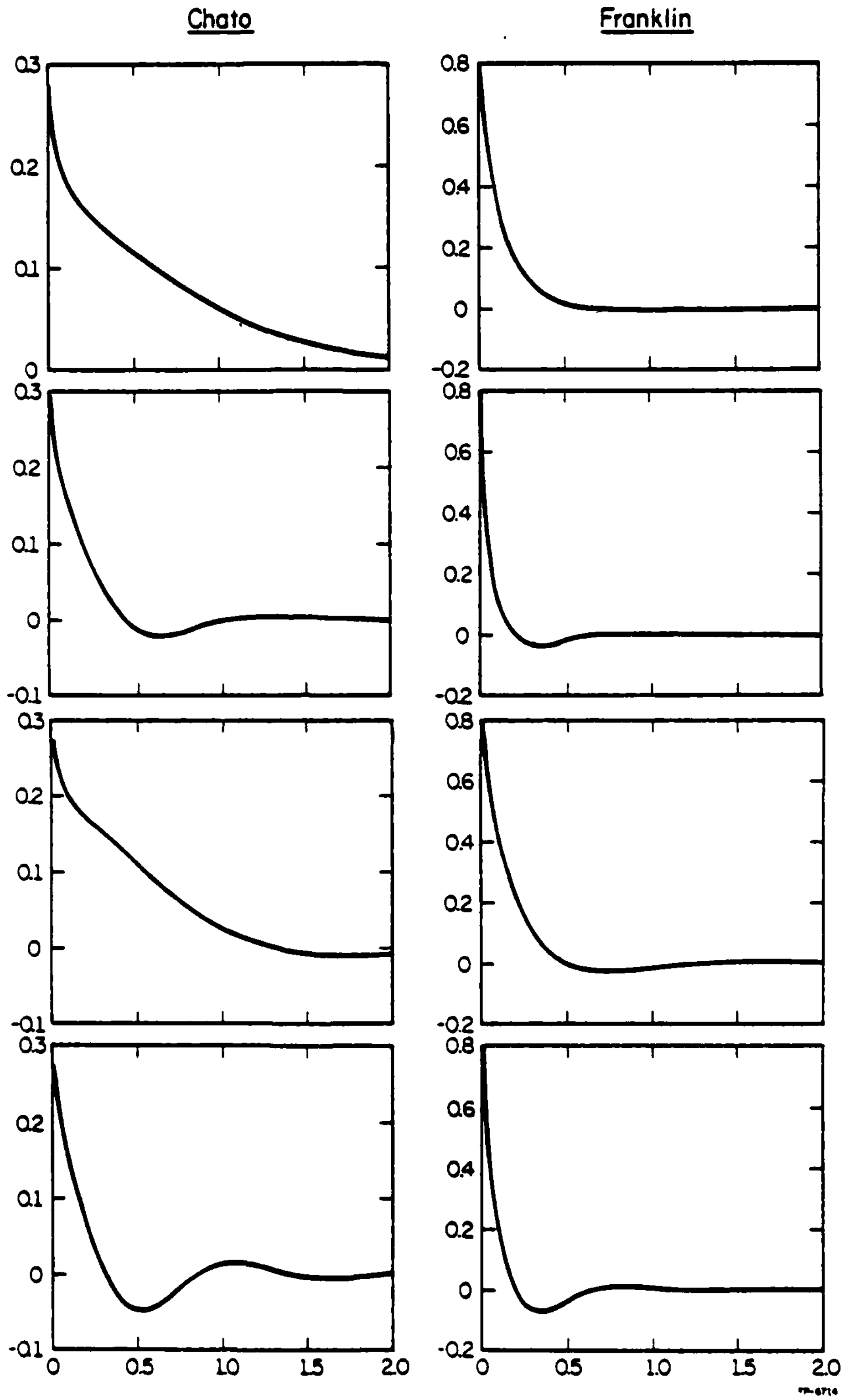

Figure 9. Control inputs for two designs.

axis in the gain space. For the problem with only the first two states available for feedback, this means no set of gains satisfying the constraints is robust with respect to the failure of either sensor.

In light of the results of [12], the problem of a robust controller was considered for the case with three feedback gains. For flight condition 4, a fixed gain using only the first two states was found which satisfied all the constraints and was robust with respect to either the first, the second, or both sensors failing. Adding the third gain set equal to zero, yields a set of three gains which is completely robust. However, this result is not surprising since the open loop poles for flight condition 4 (see Table 2) already satisfy the emergency specifications (see Figure 5 and Table 4). For the other three flight conditions considered individually, no gains could be found which were robust with respect to the first sensor failing. Thus none could be found for all the flight conditions taken together. When considered individually, a set of gains which is robust with respect to the failure of the second sensor was found for each flight condition. A set of gains which is robust with respect to the second sensor failing was also found when the first three flight conditions were considered together (see Table 7). Unfortunately, when all four flight conditions were considered, no common solution which was robust with respect to the second sensor could be found. A solution which is robust with respect to the third sensor failing is just the solution given in Table 5 with a third gain equal to zero added. These results seem to indicate that a fixed gain controller is not adequate to satisfy the robustness requirements for this example.

While studying this example, some of the problems in implementing the algorithm for the second order example in Section 5 were also problems

Table 7. Minimum energy feedback gains which are robust with respect to the failure of the second sensor (for the first 3 flight conditions only)

$\underline{k} = [-5.0138477\times10^{-2} \quad -4.0115944\times10^{-1} \quad 5.0676513\times10^{-1}]$		
Flight Condition #	Sensor #2	Closed Loop Eigenvalues
1	NF	-2.7084034, -2.0196952, -23.109953
	F	$-.72136579 \pm j1.3337152$, -26.395321
2	NF	$-4.0968046 \pm j5.1326$, -29.668796
	F	$-.77106637 \pm j5.0911232$, -36.320273
3	NF	$-1.8964697 \pm j1.7951444$, -22.887455
	F	$-.49872359 \pm j2.0622586$, -25.682948

NF: Sensor #2 has not failed

F: Sensor #2 has failed

for this example. First, the gradient of the cost with respect to the feedback gains is discontinuous at a double real pole (see Section 4). For the minimum energy gains in Table 5, the eigenvalues of the first flight condition seem to be converging to a double real pole on the boundary of the constraints. Since the gradient is discontinuous at this point, it was necessary to try initial guesses for $\underline{k}$ close to the apparent solution but on both sides of the discontinuity to be sure the algorithm was not hanging up there. The algorithm converged back to the double pole from both directions indicating that that point was indeed the solution. Also, an intellegent initial guess for $\underline{k}$ was important in order to avoid being hung up at the double root boundaries away from the solution. In that case, a pole placement which places the poles on the opposite side of the double root boundary could be done. Using those gains as a new starting point might allow the algorithm to converge to the real solution.

Another observation was that the value chosen for c' in (37) affected the final solution returned by the algorithm. For large values of c' (200-2000), the algorithm converged quickly to the boundary of the constraint region, but had trouble moving along the boundary to the minimum with iterations over $\underline{d}$ (35)-(36). As explained in Section 3, this is due to the ill conditioning of the Hessian for large values of c'. For smaller values of c', the minimization over $\underline{k}$ converged to a solution outside the boundary of the constraint region. The maximization over $\underline{d}$ forced the solution to the boundary. For this particular example, choosing c' equal to a small number for the initial iteration over $\underline{k}$ and then increasing it gradually for subsequent iterations to enforce the constraints more quickly seemed to work well. The results in this section are for c' equal to 1 for the initial iteration and doubled thereafter.

Summarizing the results of this section, the algorithm developed in this thesis was applied to the problem of designing a controller for the F4-E aircraft. A fixed gain controller was found which satisfied the design specifications under normal operating conditions. However, a fixed gain controller which was robust to either sensor failure was not possible. This example also served to re-emphasize some of the inherent problems with this design technique: the discontinuities of the gradient, the initial guess for $\underline{k}$, and the choice of c'.

8. CONCLUSION AND SUMMARY

This thesis has dealt with one method of solving the problem of designing a fixed gain controller for a linear time invariant system when some of the design criteria are represented as constraints on the location of the closed loop system eigenvalues in the complex plane and others are represented by a quadratic cost function which is to be minimized. First, the original problem (1)-(5) is reformulated to yield (6)-(12). In the latter form, the cost function is easier to calculate. Second, problem (6)-(12) is solved by an augmented Lagrangian method. The problem is a max-min problem. A variable metric method is used to solve the minimization over $\underline{k}$. A fixed step size method is used to solve the maximization over $\underline{d}$ [19]. Third, expressions for the gradients needed to solve (32)-(34) are derived.

Two examples are studied: a simple second order numerical example and a model of the longitudinal motion of a F4-E plane. Both examples serve to point out several problems with implementing the solution of (32)-(34). First, there are discontinuities in the gradients for the case when a complex pair of system poles change to a real pair or vice versa. If the algorithm gets hung up at such a point, a new starting point on the other side of the boundary may help. Second, the value of c' in (34) must be chosen appropriately for a given problem. Too large a value of c' causes slow convergence of the algorithm. Too small a value yields a solution outside the boundary. The best approach seems to be to choose c' small for the first iteration and increase it thereafter. Finally, a good initial guess for $\underline{k}$ is important in order for the algorithm to converge properly.

There are advantages to this design method. First, it has the ability to incorporate diverse design criteria such as minimum energy control, rate of change of input, constraints on the location of poles in the complex plane, etc. Second, multi-input, multi-output systems can be considered (at least in theory). Third, it has the ability to handle larger systems than some of the other methods used to solve this type of problem. Finally, it provides insight into the effects of the various design constraints. It can be used to determine which of the design specifications can be satisfied and which ones may be too stringent.

REFERENCES

1. J. Ackermann, "Parameter Space Design of Robust Control Systems," Proc. of the JACC, Denver, Colorado, June 1979.

2. H. R. Sirisena and S. S. Choi, "Pole Placement in Prescribed Regions of the Complex Plane Using Output Feedback," IEEE Trans. on Automatic Control, Vol. AC-20, No. 6, December 1975.

3. A. Schy, W. M. Adams, and K. A. Johnson, "Computer Aided Design of Control Systems to Meet Many Requirements," AGARD Conf. Proc. on Advances in Control Systems, No. 137, Geilo, Norway, 1973, pp. 6.1-6.7.

4. R. E. Kalman, "When is a Linear Control System Optimal?," Trans. ASME (J. Basic Engr.), 1964, pp. 51-60.

5. B. D. O. Anderson and J. B. Moore, Linear Optimal Control, Prentice-Hall, Englewood Cliffs, N.J., 1971.

6. M. Safonov and M. Athans, "Gain and Phase Margin for Multiloop LQG Regulators," IEEE Trans. on Automatic Control, 1977, pp. 173-179.

7. C. A. Harvey and R. E. Pope, "Study of Synthesis Techniques for Insensitive Aircraft Control Systems," NASA Contractor Report CR-2803, April 1977.

8. C. A. Harvey and R. E. Pope, "Insensitive Control Technology Development," NASA Contractor Report 2947, February 1978.

9. A. Vinkler and L. Wood, "A Comparison of Several Techniques for Designing Controllers of Uncertain Dynamic Systems," Proc. of 17th IEEE Conf. on Decision and Control, San Diego, Calif., January 1978, pp. 31-38.

10. V. Zakian and U. Al-Naib, "Design of Dynamical and Control Systems by the Method of Inequalities," Proc. IEEE, Vol. 120, 1973, pp. 1421-1427.

11. A. Kreisselmeier and R. Steinhauser, "Systematic Control Design by Optimizing a Vector Performance Index," Proc. IFAC Symp. on Computer-Aided Design of Control Systems, Zurich, August 1979.

12. S. N. Franklin, "Design of a Robust Flight Control System," M.S. thesis, University of Illinois, Urbana, 1979.

13. D. P. Looze, "Decomposition of Linear Decentralized Stochastic Control Problems," Ph.D. thesis, MIT, Cambridge, Mass., September 1978.

14. R. Brockett, Finite Dimensional Linear Systems, Wiley, New York, 1970.

15. D. G. Luenberger, Introduction to Linear and Nonlinear Programming, Addison-Wesley, Rading, Mass., 1973.

16. W. S. Levine, "Optimal Output-Feedback Controllers for Linear Systems," Ph.D. thesis, MIT, Cambridge, Mass., 1969.

17. M. R. Hestenes, "Multiplier and Gradient Methods," Journal of Optimization Theory and Applications, Vol. 4, No. 5, 1969.

18. D. P. Bertsekas, "Combined Primal-Dual and Penalty Methods for Constrained Minimization," SIAM J. Control, Vol. 13, No. 3, May 1975.

19. D. B. Bertsekas, "On the Method of Multipliers for Convex Programming," IEEE Trans. on Automatic Control, Vol. AC-20, No. 3, June 1975.

20. J. E. Dennis and H. H. W. Mei, "An Unconstrained Optimization Algorithm which Uses Function and Gradient Values," Technical Report TR 75-246, Dept. of Computer Science, Cornell University, Ithaca, NY, June 1975.

21. J. E. Ackermann, "A Robust Control System Deisgn," Proc. JACC, Denver, Colo., 1979.

22. J. B. Mankin, A Study of Control System Sensitivity, Management Information Services, Detroit, Michigan, 1972.

23. R. L. Berger, J. R. Hess, and D. C. Anderson, "Compatibility of Maneuver Load Control and Relaxed Static Stability Applied to Military Aircraft," AFFDL-TR-73-33, April 1973.

24. H. Kwakernaak and R. Sivan, Linear Optimal Control Systems, Wiley-Interscience, New York, 1972.

DATE
ILME

-8